Aberrant Chondrocyte Hypertrophy and Activation of ß-Catenin Signaling Precede Joint Ankylosis in *ank/ank* Mice

FACUNDO LAS HERAS, KENNETH P.H. PRITZKER, ANTHONY SO, HING WO TSUI, BASIL CHIU, ROBERT D. INMAN, and FLORENCE W.L. TSUI

ABSTRACT. ***Objective.*** We assessed the role of *Ank* in the maintenance of postnatal articular cartilage using the *ank/ank* mouse (mice homozygous for *progressive ankylosis*).

Methods. We analyzed *ank/ank* mice and wild-type littermates (8, 12, and 18 weeks old). Sections from decalcified, paraffin-embedded joints were stained with hematoxylin and eosin. Articular chondrocyte size and cartilage thickness were determined using morphometric methods. Immunohistochemical staining was performed with anticollagen X, antitissue nonspecific alkaline phosphatase (TNAP), and anti-ß-catenin antibodies on fixed joint sections. Axin2 expression in paw joint lysates in wild-type versus *ank/ank* mice were compared using Western blot analysis.

Results. In all age groups of normal mice studied, calcified cartilage (CC) chondrocyte areas were significantly larger than those of uncalcified cartilage (UC) chondrocytes. However, similar chondrocyte areas (UC vs CC) were found in 12-week and 18-week-old *ank/ank* mice, indicating that hypertrophic chondrocytes were present in the UC of these mutant mice. The *ank/ank* mice showed an increase in CC thickness. The *ank/ank* UC hypertrophic chondrocytes showed diffuse immunoreactivity for collagen X and TNAP. Increased ß-catenin activation was demonstrated by nuclear localization of ß-catenin staining in *ank/ank* chondrocytes. Axin2 expression from paw lysates was downregulated in *ank/ank* mice.

Conclusion. We identified a previously unrecognized phenotype in the articular cartilage of *ank/ank* mice: collagen X-positive hypertrophic chondrocytes in the UC. It is possible that consequent to downregulation of axin2 expression, ß-catenin signaling was activated, leading to accelerated chondrocyte maturation and eventual ankylosis in *ank/ank* joints. Our studies shed new light on the contribution of a key signaling pathway in this model of joint ankylosis. (J Rheumatol First Release Feb 1 2012; doi:10.3899/jrheum.110971)

Key Indexing Terms:
CHONDROCYTE HYPERTROPHY ß-CATENIN SIGNALING ank MOUSE
OSTEOARTHRITIS ANKYLOSING SPONDYLITIS

Inorganic pyrophosphate (PPi) metabolism is common to all cells and plays an important role in regulating mineralization and bone formation. PPi in the cartilage extracellular matrix (ECM) is exported by the Ank/ANKH protein[1] and generated by ectonucleotidases, mainly ENPP-1[2,3]. The mouse mutant *Ank* (*progressive ankylosis*) has a loss-of-function mutation in the *Ank* gene[1]. Although *Ank* is expressed in embryonic cells, *ank/ank* mice are normal at birth. It is possible that ENPP-1 compensates for *Ank* functions in embryonic development and early postnatal state. Adult *ank/ank* mice have pathologic calcium apatite crystal deposition and eventual bony ankylosis of the affected joints[4]. Mice with joint-specific deletion of *Ank* alleles also show joint mineralization and ankylosis[5], indicating that *Ank* functions locally in joints. In fact, *Ank* gene expression is at least 16-fold higher in surface articular chondrocytes compared to the level expressed in growth plate chondrocytes[6], suggesting that *Ank* has important functions in articular cartilage. The best documented function of *Ank* relates to the regulation of intracellular and extracellular PPi levels[1,7]. Other functions of *Ank* include regulating early erythroid[8] and osteoblast/osteoclast differentiation[9,10].

Modulators of *Ank* expression have been reported. For

From Pathology and Laboratory Medicine, Mount Sinai Hospital, and the Department of Laboratory Medicine and Pathobiology, University of Toronto; the Genetics and Development Division, Toronto Western Research Institute, University Health Network; and the Department of Immunology, University of Toronto, Toronto, Ontario, Canada.

Supported by grants from the Canadian Institutes of Health Research, the Arthritis Center of Excellence, The Arthritis Society, and Pathology and Laboratory Medicine, Mount Sinai Hospital.

F. Las Heras, MD, PhD, Pathologist; K.P.H. Pritzker, MD, BSc(Med), FRCPC, Pathologist in Chief, Mount Sinai Hospital; A. So, BSc, Medical Student, University of Toronto; H.W. Tsui, PhD, Research Associate; B. Chiu, PhD, Research Associate; R.D. Inman, MD, FRCPC, FACP, FRCP Edin, Deputy Physician in Chief, Research, Rheumatologist, Senior Scientist; F.W.L. Tsui, PhD, Senior Scientist, Toronto Western Research Institute.

Dr. F.W.L. Tsui and Dr. R.D. Inman are both senior authors of this report.

Address correspondence to Dr. F.W.L. Tsui, Toronto Western Hospital, Mc14-419, 399 Bathurst Street, Toronto, Ontario M5T 2S8, Canada. E-mail: ftsui@uhnres.utoronto.ca

Accepted for publication October 26, 2011.

example, *Ank* expression is lower in hypoxic environments such as growth plate and articular cartilage, while higher expression has been found in the synovium and meniscus with normoxic conditions[11]. In rat chondrocytes, transforming growth factor-ß (TGF ß) induced *Ank* expression through the Ras/Raf-1/ERK and calcium-dependent protein kinase C pathways, leading to PPi export to the extracellular matrix[12].

In view of the fact that *Ank* mice are outbred and our colony of *Ank* mice originated from a breeding pair derived from frozen embryos, we characterized the phenotypes of our *ank*/*ank* mice. We report the detection of a previously unrecognized phenotype in the articular cartilage of *ank*/*ank* mice, namely the presence of hypertrophic chondrocytes in the uncalcified cartilage (UC). We show that ß-catenin signaling is involved in the development of this phenotype.

MATERIALS AND METHODS

Ank mice. A breeding pair of heterozygous ank mice (C3FeB6-A/A$^{w\text{-}j}$ - *ank*$^{+/-}$) was purchased from Jackson Laboratory (Bar Harbor, ME, USA). Mice were genotyped using tail DNA as described by Ho, *et al*[1]. More than 50 mutant mice were evaluated. For histomorphometry, 4 mutant female (*ank*/*ank*) mice and 4 normal female littermate controls were analyzed for each age group (8, 12, and 18 weeks, except for 3 *ank*/*ank* mice who were 18 weeks old). Female mice were used exclusively in our study because the clinical phenotype in them is more severe than in male mice in our colony. All animal procedures were approved by the institutional Animal Experimentation Committee.

Histology and cartilage morphometry. Decalcified fixed knee joint sections (5 μm) were stained with H&E. A Visiopharm Integrator System (Visiopharm Inc., Hoersholm, Denmark) was used for morphometry. For each mouse, the UC and calcified cartilage (CC) thickness of 1 knee joint was measured at 5 equidistant points across the area of interest. UC thickness was measured from the cartilage just beside the synovial space to the tidemark. CC thickness was measured from the tidemark to the edge of the subchondral bone. The mean UC/CC thickness of each mouse was used for statistical analyses. Within the cartilage from the 3 midpoints, chondrons with an intact nucleus, cytoplasm, and lacunae were evaluated. Each chondron was individually masked to obtain chondrocyte area by imaging (Figure 1). All the chondrocytes in the central 50% of the tibial plateau (~ 200 chondrons) from each of the UC or CC for each mouse were measured. The mean chondrocyte area (from UC or CC) of each mouse was used for statistical analyses.

Immunohistochemistry. Sections were treated with pepsin for antigen retrieval and 3% hydrogen peroxide to block endogenous peroxidase. The sections were stained either with anticollagen X (at 1:125 and 1:250 dilutions; Ibex Pharmaceuticals Inc., Montreal, QC, Canada) or with antitissue nonspecific alkaline phosphatase (TNAP; at 1:10 dilution) or with anti-ß-catenin (at 1:400 dilution) antibodies. MM-horseradish peroxidase (HRP) polymer was used as a detection system (BioCare-UK, Birmingham, UK), visualized with diamino-benzidine methods (Vectastain DAB Kit, Vector Laboratories, Burlingame, CA, USA). Sections were counterstained with Mayer's hematoxylin. Positive and negative controls were stained in parallel. Specificity of the staining was verified each time using the same isotypic antibody as a control. For assessing the percentage of articular chondrocytes with nuclear localization of ß-catenin, ~ 200 chondrocytes from 1 knee joint of each mouse (four 14-week-old mice each from both wild-type and *ank*/*ank* mice) were counted.

Immunoblotting. Skin from front paws of mice was removed. Interphalangeal joints from the front paws were solubilized in 6 M urea. Lysates with sodium dodecyl sulfate (SDS) and dithiothreitol were boiled for 3 min, loaded and run on SDS-PAGE, and transferred to Immobilon-P transfer membrane. After blocking with 3% bovine serum albumin in Tris-buffered saline with Tween 20 (10 mM Tris pH8, 500 mM NaCl, 0.1% Tween 20) for 1 h, the blots were incubated with either a mouse monoclonal antibody to *Escherichia coli* ß-galactosidase (ß-gal) or a goat anti-axin2 antibody (both from Santa Cruz Biotechnology, Santa Cruz, CA, USA) or a monoclonal anti-ß-actin antibody for 45 min and then with HRP-conjugated antigoat or antimouse antibody (Jackson) for 30 min. Specific signals were detected by chemiluminescence using Supersignal West Femto maximum sensitivity substrates (Pierce Biotech, Rockford, IL, USA) and imaging.

Statistical analysis. Data from the different groups (4 mice in each group and three 18-week *ank*/*ank* mice) were compared using the nonparametric Mann-Whitney U test (SPSS v 16.0). P values < 0.05 were considered significant. Results were expressed as mean with 95% CI and were presented using box plots.

Generation of TOPGAL ank/ank mice. *TOPGAL* mice were purchased from Jackson Laboratory. Heterozygous *Ank* mice (homozygous mutants are infertile) were crossed with *TOPGAL* mice bearing the ß-gal transgene driven by a T cell factor (TCF) ß-catenin responsive promoter. F1 progenies bearing the transgene were intercrossed to generate *TOPGAL ank*/*ank* mice. Genotyping for the transgene was carried out as described in Hens, *et al*[13]. *Ank*/*ank* mice with and without the transgene exhibit similar phenotypes (data not shown).

RESULTS

Radiology and histopathology. Progressive radiographic changes were detected in the menisci and the patella of *ank*/*ank* knees (Figure 2B). Axial joint abnormalities included syndesmophytes at costosternal junctions and extensive marginal syndesmophyte formation (Figure 2C, arrows) between vertebral bodies ("bamboo" spine). Histologically, these syndesmophytes were represented by proliferating osteoblasts and differentiated osteocytes in a mature bone matrix (Figure 2D, thick arrow). Calcium hydroxyapatite crystals were present in the intervertebral space (Figure 2D, dashed arrow). A large number of hypertrophic chondrocytic-like cells were detected in the proximity of new bone formation (Figure 2D, thin arrow). No inflammation was observed.

Morphometry of chondrocytes in the knee joints. As observed by Sampson[14], the peripheral joints of *ank*/*ank* mice showed proliferation of the fibroblast-like synoviocytes (Figures 3A and 3B; arrows). In contrast to previous reports showing a mononuclear inflammatory infiltrate in synovia[4], no inflammation was seen in our *ank*/*ank* mice at any age.

Detailed examination of the UC revealed chondrocyte hypertrophy in *ank*/*ank* mice compared with wild-type controls (Figures 4A and 4B). Normally, hypertrophic chondrocytes are never found in UC and thus one would expect a significant difference in the UC versus CC chondrocyte area in the articular cartilage of normal mice. Indeed, in all 3 age groups of normal mice, average CC chondrocyte areas were significantly larger than those of UC chondrocytes ($p = 0.021$ for all age groups). Significant differences in average chondrocyte areas were also detected in 8-week *ank*/*ank* UC versus CC ($p = 0.021$). However, similar mean chondrocyte

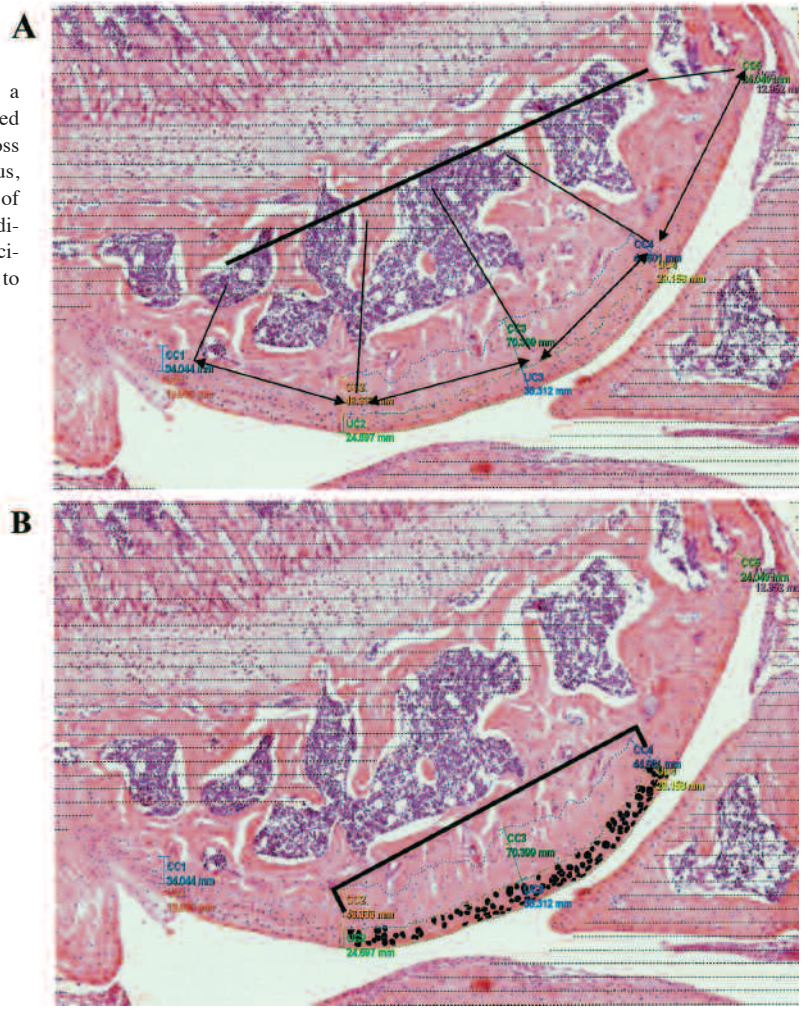

Figure 1. Histomorphometric analysis of knee joints using a Visiopharm Integrator System. A. The thickness of the uncalcified and calcified cartilage was measured at 5 equidistant points across the area of interest. B. Chondrons showing an intact nucleus, cytoplasm, and lacunae were evaluated in the central 50% of uncalcified and calcified cartilage. Each chondrocyte was individually masked (for example, blackened cells represent uncalcified cartilage chondrocytes) and image analysis was performed to obtain chondrocyte area.

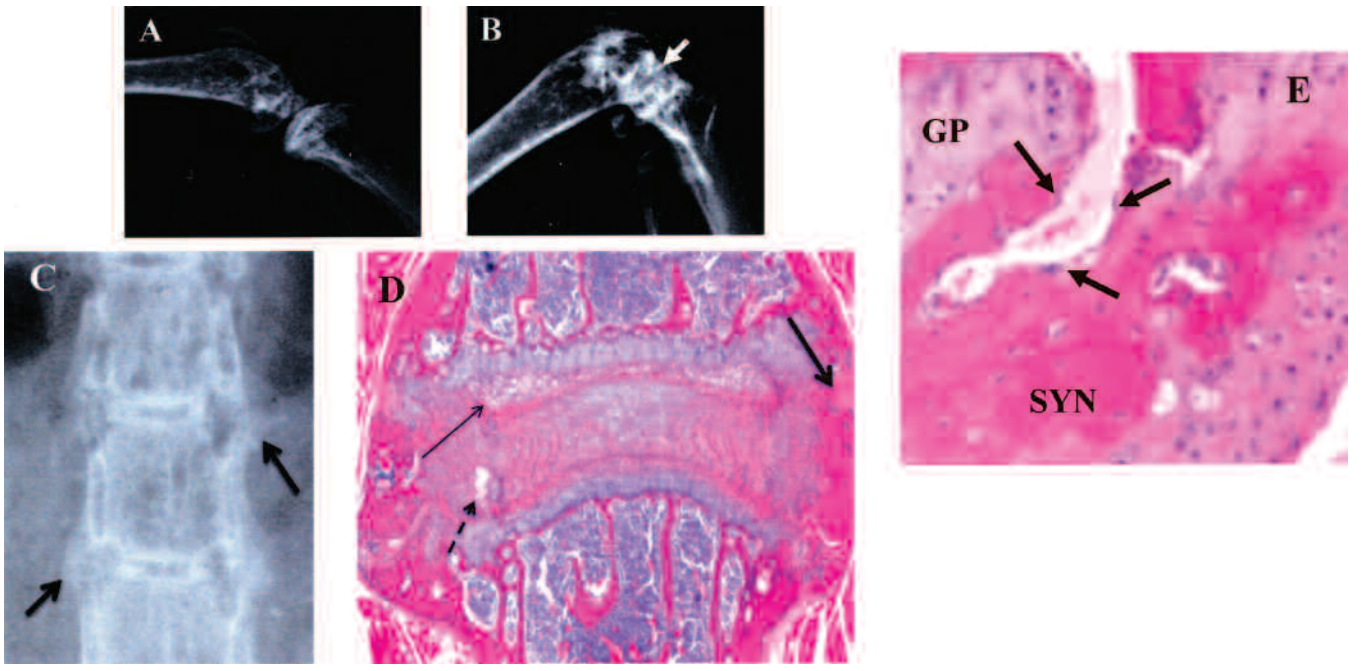

Figure 2. Radiographic and histological evaluation of joints from wild-type (wt) and *ank/ank* mice. A. Radiograph showing knee joint of a wt mouse (12 weeks). B. Radiograph showing knee joint of an ank/ank mouse (18 weeks). Arrow shows extensive calcification and complete knee joint ankylosis. C. Radiograph of *ank/ank* spine (12 weeks) showing bridges of new bone formation (syndesmophytes) extending from 1 vertebral edge to another (arrows). D. Histological section of *ank/ank* syndesmophyte, showing bridges of mature bone formation (thick arrow) and hydroxyapatite crystals (dashed arrow). Hypertrophic chondrocytes are identified in the vicinity of new bone formation areas (thin arrow). E. A higher magnification image of an *ank/ank* syndesmophyte (SYN) showing proliferating osteoblasts (arrows). GP: growth plate.

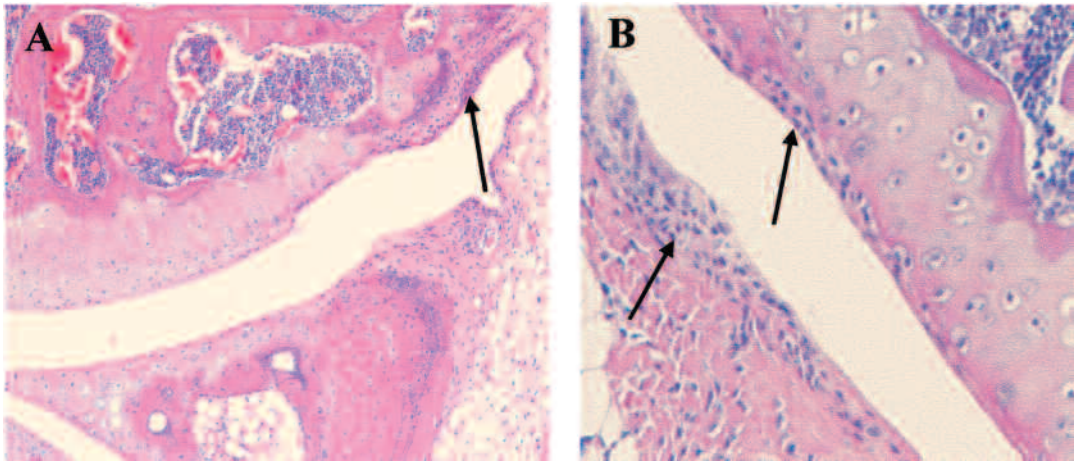

Figure 3. Histological features of *ank/ank* articular joints. A. The cartilage layer is intact with no signs of infiltration in the joint space. Arrow shows proliferating fibroblast-like synoviocytes. B. A higher-power image showing the absence of leukocyte infiltrates in synovial hyperplasia (arrows).

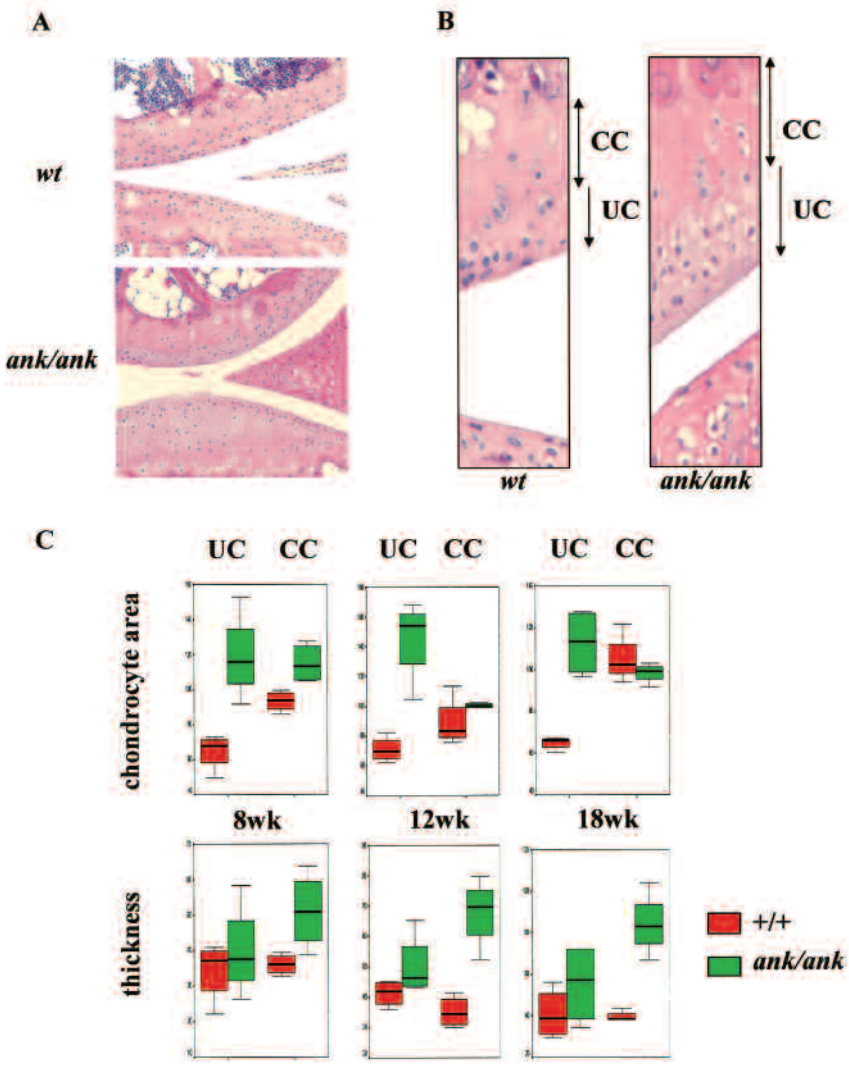

Figure 4. Articular cartilage from wild-type (wt) versus *ank/ank* mice. A. Histological evaluation of articular cartilage from wt versus *ank/ank* mice (both 18 weeks of age). *Ank/ank* joints showed joint space narrowing and amorphous debris within the joint space. B. Detailed histological features of articular cartilage from the knee joint of wt versus *ank/ank* mice (both 12 weeks of age). UC: uncalcified cartilage; CC: calcified cartilage. C. Box plots comparing UC versus CC chondrocyte area (top panels), UC versus CC thickness (bottom panels) of wt mice (red boxes) versus *ank/ank* mice (green boxes) at ages 8, 12, and 18 weeks.

areas (UC vs CC) were found in 12-week and 18-week *ank/ank* articular cartilage (p values were nonsignificant), indicating that hypertrophic chondrocytes were present in the articular UC of 12-week and 18-week *ank/ank* mice (Figure 4C).

There was a progressive increase in the CC thickness in *ank/ank* mice, compared to that of wild-type mice. In wild-type articular cartilage, there was no significant difference between the UC versus CC thickness in all 3 age groups. In contrast, in all 3 age groups of *ank/ank* articular cartilage, CC thickness was significantly greater than that of UC (Figure 4C).

Immunohistochemical (IHC) studies of the knee joints. In wild-type mice, collagen X expression, a marker for hypertrophic chondrocytes, was detected primarily in the hypertrophic chondrocytes in the articular CC (Figure 5A), and was not detected in the uncalcified chondrocytes. In contrast, chondrocytes from the UC of *ank/ank* mice showed membrane and cytoplasmic reactivity for collagen X, and hypertrophic chondrocytes from the CC were also positive (Figure 5B). A semiquantitative analysis of collagen X positivity, using 2 different antibody concentrations, indicated that collagen X protein expression was more than 2-fold higher in the articular hypertrophic chondrocytes from *ank/ank* mice, compared to wild-type mice.

TNAP has long been regarded as a marker of chondrocyte hypertrophy[15]. We recently showed that dysregulation of *Ank* gene expression affected TNAP expression and activities[16]. Thus, we carried out IHC studies of the *ank/ank* versus normal knee joints using an anti-TNAP antibody. TNAP staining was consistently higher in the articular hypertrophic chondrocytes from the *ank/ank* UC (Figure 5D). As expected, normal articular cartilage had only focal TNAP positivity in the uncalcified layer (Figure 5C).

Activation of ß-catenin signaling in ank/ank chondrocytes. Canonical wingless (Wnt)/ß-catenin signaling is involved in bone formation remodeling during growth and development and in the postnatal state[17]. Activation of this signaling pathway in mature chondrocytes stimulates hypertrophy and matrix mineralization[18]. *Ank/ank* mice and ß-catenin conditional activation (cAct) mice[19] share a common hypertrophic chondrocyte phenotype in the postnatal articular cartilage. Thus we asked whether ß-catenin signaling is dysregulated in *ank/ank* mice. IHC studies of *ank/ank* versus normal knee joints using an anti-ß-catenin antibody showed nuclear localization of ß-catenin (a marker for activation of ß-catenin signaling) in *ank/ank* articular chondrocytes. In young normal mice (up to 8 weeks of age), ß-catenin staining was observed in the cytoplasm and membrane of articular cartilage (Figure 6A). In contrast, in young *ank/ank* mice, intense ß-catenin expression (mainly localized in the nuclei) was detected in both articular and epiphyseal chondrocytes (Figure 6B and 6D). Strong ß-catenin staining was present in the epiphyseal intercellular matrix, predominantly in the proliferating and prehypertrophic zones (Figure 6D, arrow). Weak ß-catenin staining was observed in the epiphyseal cartilage matrix from young normal mice (Figure 6C). High expression of ß-catenin was also present in the perichondrium of *ank/ank* mice (Figure 6B, arrow).

In mature normal mice (12–17 weeks old), little or no ß-catenin staining was detected in the superficial layer of articular chondrocytes, epiphyseal chondrocytes, matrix, or perichondrial cells (Figures 7A and 7D). Focal positive staining was observed only in the deep layer of chondrocytes in the articular cartilage (Figure 7A) and the trabecular bone (Figure 7D). In contrast, strong cytoplasmic and nuclear ß-catenin staining persisted in all layers of the articular cartilage from mature *ank/ank* mice (Figure 7B). In 14-week-old normal mice, 8% of articular chondrocytes (2.6–13.4%; n = 4 mice; UC chondrocytes counted from 1 knee joint of each mouse) showed nuclear localization of ß-catenin. In age-matched *ank/ank* mice, nuclear staining was found in a significantly higher percentage of articular chondrocytes (46%; 30.1–61.6%; n = 4 mice; UC chondrocytes counted from 1 knee joint of each mouse; p = 0.021; Figure 7C). Similar intense staining was present in the epiphyseal chondrocytes, cartilage matrix, and in perichondrial cells of *ank/ank* mice (Figure 7E). Syndesmophytes from the mature *ank/ank* spine showed intense ß-catenin staining in osteoblasts and in the chondrocytic-like cells in the vicinity of new bone formation (Figures 8B and 8D). Positive ß-catenin staining was present only in the CC of the vertebral bodies from the normal spine.

We unexpectedly observed positive ß-catenin staining in the ECM, especially in the growth plates (more prominent in the mutant than normal mice). Although little staining was detected in negative control sections, we cannot rule out the possibility that this finding might reflect some degree of cross-reactivity of the primary antibody used. To confirm that ß-catenin signaling was upregulated in *ank/ank* joints using an alternative approach, we generated *ank/ank* mice with a ß-gal transgene (*TOPGAL*) driven by a TCF ß-catenin responsive promoter[13]. Western blots of front paw joint lysates from *TOPGAL*-positive versus *TOPGAL ank/ank* mice (two 12-week mice each) were probed with an antibody to bacterial ß-gal, and ß-actin expression was used as a normalization marker. Higher ß-gal signals were detected in lysates from *TOPGAL ank/ank* mice (Figure 9A).

Role of axin2 in the development of the hypertrophic chondrocyte phenotype in ank/ank mice. Axin2 is a negative regulator of canonical Wnt/ß-catenin signaling[20]. It is also a concentration-limiting factor in the ß-catenin degradation complex[21,22]. In view of the fact that disruption of axin2 expression resulted in accelerated chondrocyte maturation[23], we assessed whether axin2 expression was dysregulated in *ank/ank* joints. Because posttranscriptional regulation plays an important role in proteins that participate in ß-catenin signaling, we compared the levels of axin2 pro-

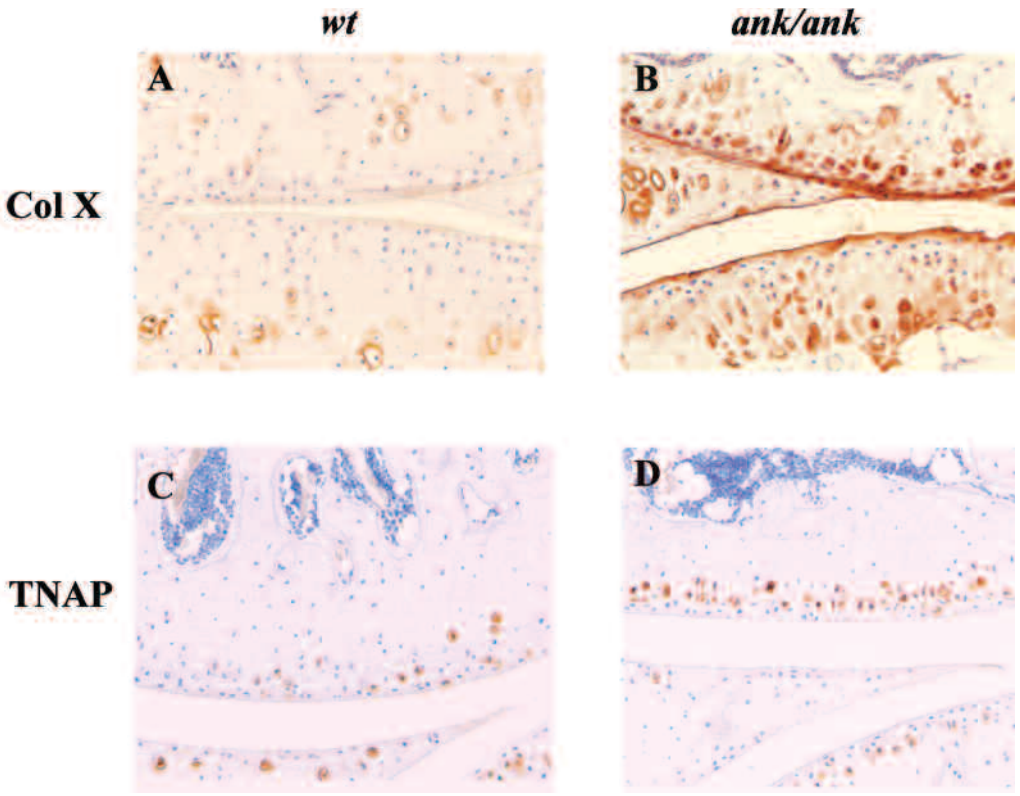

Figure 5. Immunohistochemical staining of collagen X (Col X) and tissue nonspecific alkaline phosphatase (TNAP) of wild-type (wt) versus *ank/ank* articular joint sections. A. The wt joint section was incubated with anticollagen X antibody at 1:125 dilution. B. The *ank/ank* joint section was incubated with the same antibody at 1:250 dilution. C. The wt joint section was stained with anti-TNAP antibody. Only focal chondrocytes from the calcified cartilage showed positive staining. D. The *ank/ank* joint section was stained with anti-TNAP antibody. Accentuated TNAP staining was detected in both uncalcified and calcified articular chondrocytes.

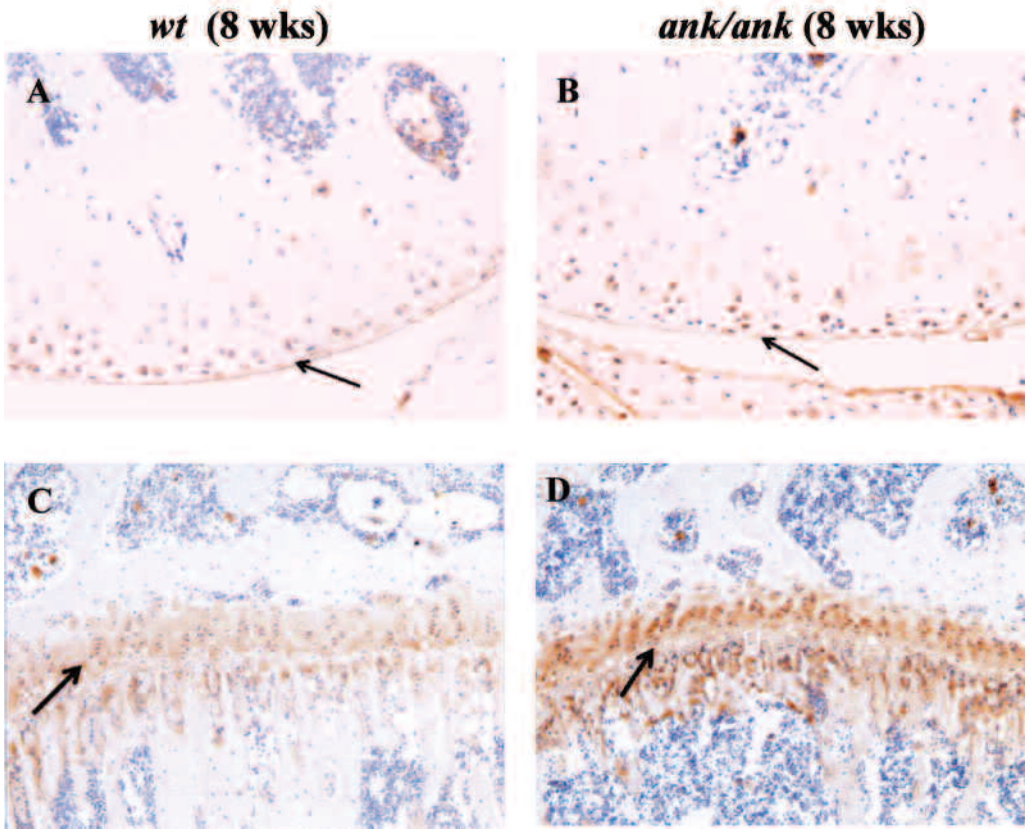

Figure 6. Immunohistochemical staining of ß-catenin in articular and epiphyseal cartilage of wild-type (wt) versus *ank/ank* mice (both 8 weeks old). A. Weak cytoplasmic and membrane staining of the articular cartilage of wt mice. B. Strong ß-catenin staining in *ank/ank* articular chondrocytes with nuclear localization. Arrow shows higher expression of ß-catenin in the *ank/ank* perichondrium. C. Weak cytoplasmic and membrane staining (arrow) of the epiphyseal cartilage of wt mice. D. Prominent ß-catenin staining in *ank/ank* epiphyseal cartilage, mainly in the proliferating and prehypertrophic zones (arrow) and the epiphyseal intercellular matrix.

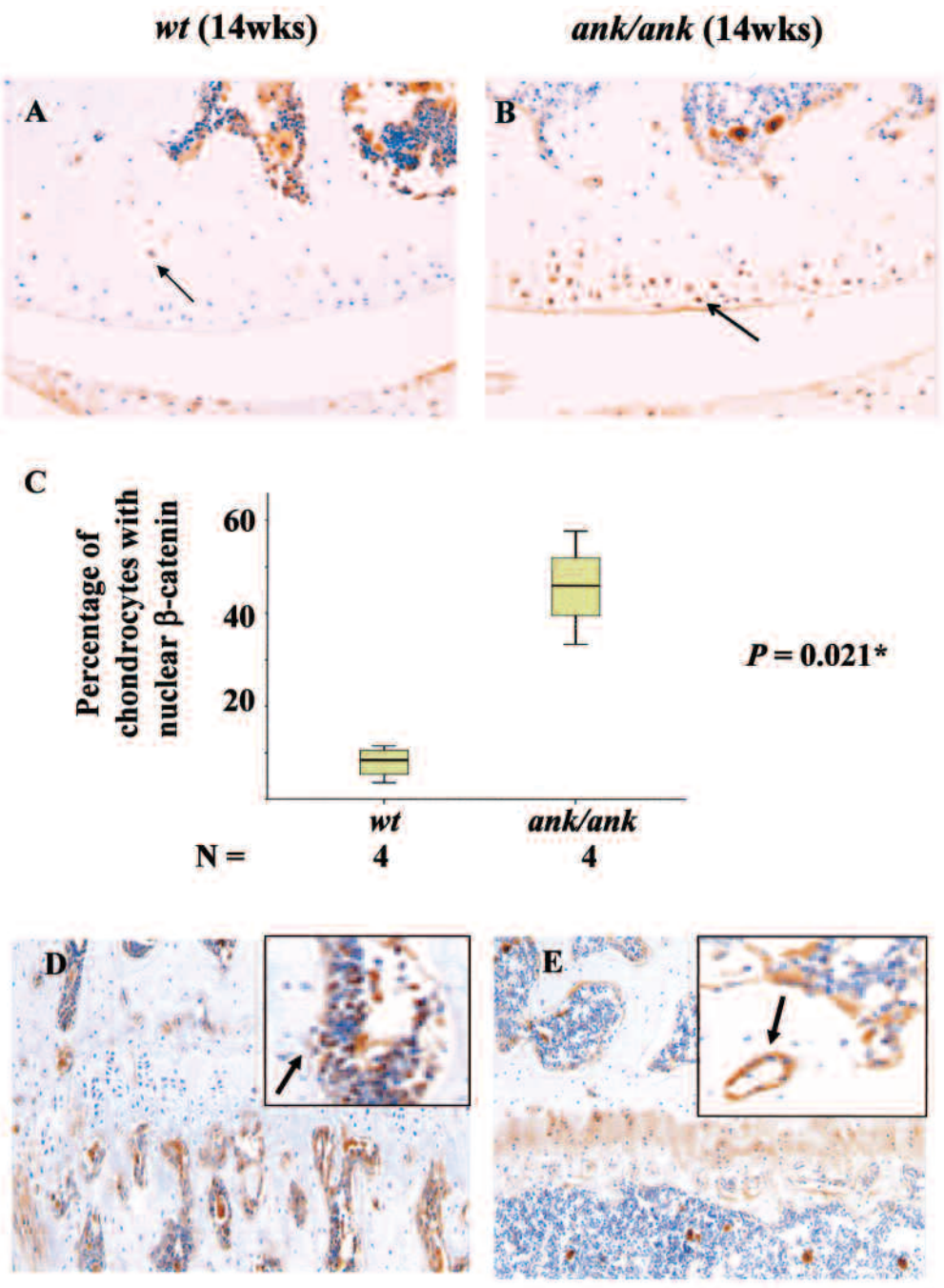

Figure 7. Immunohistochemical staining of ß-catenin in articular and epiphyseal cartilage of wild-type (wt) versus *ank/ank* mice (both 14 weeks old). A. In mature wt joint sections, little or no ß-catenin staining (arrow) in the superficial layers of articular chondrocytes. B. Mature *ank/ank* articular cartilage showed strong cytoplasmic and nuclear staining (arrow). C. Box plot comparing the percentage of articular chondrocytes with nuclear ß-catenin staining in wt versus *ank/ank* knee joints (14 weeks old, n = 4 for both groups). Mann-Whitney U test showed significant differences (*p = 0.021). D. No ß-catenin staining observed in the epiphyseal chondrocytes from mature wt mice. Only focal staining was observed in the trabecular bone (arrow in insert). E. Marked staining was present in the epiphyseal chondrocytes and cartilage matrix of mature *ank/ank* mice. B-catenin staining was detected in osteoblasts and newly formed osteoid in the trabecular bone from mature *ank/ank* mice (arrow in insert).

teins in wild-type versus *ank/ank* joint lysates. Western blots of front paw joint lysates were probed with an antibody to axin2, and ß-actin expression was used as a normalization marker. Compared to those from normal littermates, there were 2- to 5-fold fewer axin2 proteins in joint lysates from *ank/ank* mice. Figure 9B shows representative results from 2 pairs of normal versus mutant mice. Quantitation of the relative levels of axin2 expression is shown in Figure 9C (n = 3 mice per group; p = 0.05).

DISCUSSION

In our study, we report a previously unrecognized phenotype in *ank/ank* mice, namely hypertrophic chondrocytes in the UC, associated with an increase in CC thickness. Although hypertrophic chondrocytes were detected in both UC and CC of *ank/ank* articular cartilage, there was no increase in the UC thickness, while CC thickness increased progressively with age. It is likely that the hypertrophic chondrocytes in the UC of *ank/ank* mice were not terminally differ-

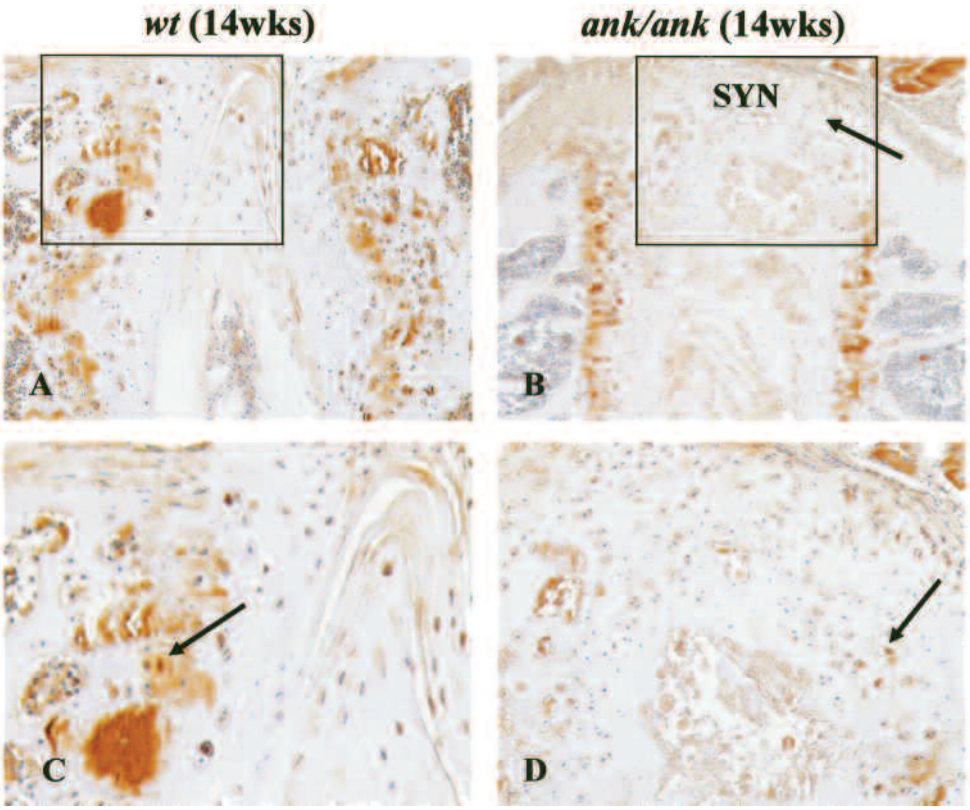

Figure 8. Immunohistochemical staining of ß-catenin in spinal articular cartilage of wild-type (wt) versus *ank/ank* mice (both 14 weeks old). A. and C. Positive staining is present mainly in deep articular cartilage from wt mice (arrow). B. and D. In *ank/ank* mice, in addition to strong signals in the growth plates, strong nuclear and cytoplasmic ß-catenin staining is detected in syndesmophytes (SYN) and areas of new bone formation associated with chondrocyte hypertrophy (arrows). Panels C and D are higher magnification images from inset areas of panels A and B, respectively.

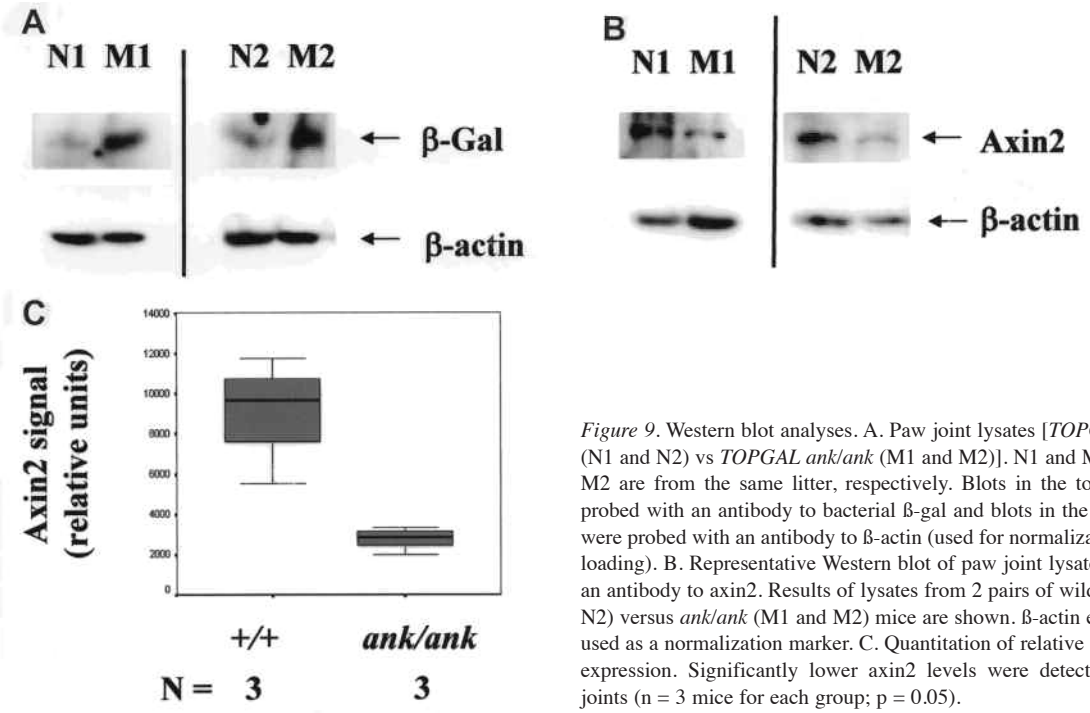

Figure 9. Western blot analyses. A. Paw joint lysates [*TOPGAL* wild-type (N1 and N2) vs *TOPGAL ank/ank* (M1 and M2)]. N1 and M1 and N2 and M2 are from the same litter, respectively. Blots in the top panels were probed with an antibody to bacterial ß-gal and blots in the bottom panels were probed with an antibody to ß-actin (used for normalization of protein loading). B. Representative Western blot of paw joint lysates probed with an antibody to axin2. Results of lysates from 2 pairs of wild-type (N1 and N2) versus *ank/ank* (M1 and M2) mice are shown. ß-actin expression was used as a normalization marker. C. Quantitation of relative levels of axin2 expression. Significantly lower axin2 levels were detected in *ank/ank* joints (n = 3 mice for each group; p = 0.05).

entiated, or inhibitory factors were present and thus ECM mineralization did not occur in the UC. We have also shown that ß-catenin signaling is activated in *ank/ank* articular cartilage and that lower axin2 protein levels are detected in *ank/ank* joint lysates. A recent study by Cailotto, *et al* showed that silencing *Ank* in rat resting articular chondrocytes mimicked the effect of interleukin 1ß on chondrocyte phenotype markers (lack of collagen X, TNAP, and runx-2 expression)[24]. Further, Wnt5a transcript was increased about 2-fold and is likely responsible for activation of the canonical Wnt-ß-catenin signaling in chondrocyte monolayer. This is an ePPi-dependent event, because exogenous PPi compensates for the *Ank*-silencing effects[18].

There are a few limitations in the Cailotto study[24]. First, our observation of the hypertrophic chondrocytes in *ank/ank* articular joints suggests that resting articular chondrocytes likely are not the predominant cell population *in vivo* when *Ank* is deficient. Second, analysis of rat resting articular chondrocytes *in vitro*[24] cannot address the consequence of activation of ß-catenin signaling in articular joints *in vivo*. Third, articular chondrocytes *in vivo* are nonproliferative and exist under hypoxic conditions. Thus, the *in vitro* systems used in the rat chondrocyte cultures[24] differ from the *in vivo* conditions. This is highly relevant because *Ank* expression is repressed in hypoxic conditions, being regulated by hypoxia-inducible factor-1[11]. In the *ank/ank* articular joints, it remains unclear whether there is upregulation of Wnt proteins. This is currently under investigation.

It is possible that in *ank/ank* joints, activation of ß-catenin signaling is consequent to lower levels of axin2, which is a negative regulator of Wnt signaling[21]. This possibility is supported by the fact that 3 mutant mice (*ank/ank*), axin2 deficient[23], and ß-catenin conditional activation (cAct) mice[19], shared a common accelerated chondrocyte maturation phenotype. It will be of interest to assess whether restoration of axin2 to its normal levels (for example, by stabilizing axin2 degradation) could modulate ß-catenin signaling in *ank/ank* chondrocytes.

It is unclear why axin2 expression is downregulated in *ank/ank* joints. Axin2 is involved in mediating the crosstalk of TGF-ß and Wnt/ß-catenin signaling[25]. There is evidence showing that *Ank* participates in TGF-ß signaling, the most compelling result being that PPi export (a known *Ank* function) was greatly diminished in TGF-ß-stimulated rat chondrocytes transfected with *Ank* small interfering RNA[24]. In postnatal mouse sternal chondrocytes, a shift from TGF-ß to Wnt/ß-catenin signaling leads to an acceleration of chondrocyte maturation[25]. This raises the possibility that aberrant TGF-ß signaling may contribute to activation of Wnt/ß-catenin signaling in *ank/ank* chondrocytes, leading to the hypertrophic chondrocyte phenotype and progressive ankylosis in the mutant mice. This notion is supported by the fact that similar to *ank/ank* mice, mice deficient in TGF-ß signaling[26,27] have hypertrophic chondrocytes in the articular UC.

There are 2 distinct joint-related phenotypes of *ank/ank* mice that mimic 2 major human rheumatic diseases: hypertrophic chondrocytes in osteoarthritic articular cartilage and the joint ankylosis of ankylosing spondylitis (AS). Canonical Wnt/ß-catenin signaling has been implicated in the pathogenesis of osteoarthritis (OA)[28]. In contrast to the *Ank*-deficient hypertrophic chondrocytes found in articular cartilage of *ank/ank* mice, the hypertrophic chondrocytes seen in OA joints showed upregulation of *ANKH* expression[29]. It appears paradoxical that increased *Ank* expression was detected in hypertrophic chondrocytes from growth plates and osteoarthritic cartilage, while hypertrophic chondrocytes were also detected in *ank/ank* articular UC where there are no functional *Ank* proteins. For systems that have feedback, loss of function and gain of function could result in a similar phenotype. A similar situation was present in mouse mutants, in which both the loss and gain of function of ß-catenin in articular cartilage resulted in a similar OA-like phenotype, but the underlying mechanisms were different[19,30].

Despite the presence of hypertrophic chondrocytes and activated ß-catenin signaling in *ank/ank* mice, unlike OA, our mutant mice do not demonstrate joint fibrillation or progressive degenerative joint disease. In prostate cancer metastatic to the bone, the outcome of the bone phenotype could be osteoinductive or osteolytic, and appeared to be determined by the presence/absence of bone morphogenetic protein and Wnt signaling antagonists[31,32]. It is tempting to hypothesize that dysregulation of these signaling antagonists leads to the development of ankylosis (rather than cartilage degradation) in *ank/ank* mice. In prior studies, both the presence of joint inflammation[4] and the lack of evidence of inflammation in the *ank/ank* joints[33] were reported. In our colony of *ank/ank* mice, there were no signs of joint inflammation, and this might explain the lack of joint destruction in our mutant mice. Unlike *ank/ank* articular cartilage, there is no increase in CC in patients with OA. These differences are expected, because OA is a complex disease involving numerous risk factors, while *ank/ank* mice have a single gene defect.

We and others showed previously that *ANKH* was modestly associated with AS[34,35], although no *ANKH* association was detected in a UK study[36]. Even if *ANKH* polymorphisms do not constitute a risk factor for AS in genetic studies, it is possible that localized dysregulation of *ANKH* occurs in AS joints, because growth factor[37] and androgen[38] influence *ANKH* expression. *Ank/ank* mice represent an informative model for the study of joint ankylosis in AS for 3 reasons, as follows: (1) Progressive joint ankylosis, both peripheral and axial, is a phenotype shared by both the *ank/ank* mice and patients with AS. (2) We showed that Wnt/ß-catenin signaling is activated in *ank/ank* joints. There is increasing evidence that this signaling pathway plays an important role in joint ankylosis in patients with AS. A recent report showed that serum Dickkopf-1 (DKK-1; a Wnt antagonist) from patients with AS is dysfunctional and thus

likely leads to neoossification in these patients through activation of the Wnt/ß-catenin signaling pathway[39]. In a murine model of sacroiliitis, blocking DKK-1 resulted in local chondrocyte hypertrophy, upregulation of type X collagen expression, and enhanced ankylosis of the sacroiliac joints[40]. The role of Wnt/ß-catenin signaling in the development of ankylosis in patients with AS is also implicated by the finding that expression of sclerostin (SOST), an antagonist of ß-catenin signaling, was undetectable in AS osteocytes[41]. And (3) the hallmark of AS is osteoproliferation at the site of inflammation. Although anti-tumor necrosis factor agents are extremely successful in controlling joint inflammation in AS, results of numerous studies have revealed that they have minimal effect on new syndesmophyte formation[42,43]. Currently, there is an active debate whether ankylosis and inflammation are uncoupled in AS[44]. The unique feature in our *ank/ank* mice (ankylosis in the absence of joint inflammation) offers an opportunity to directly separate the molecular basis underlying ankylosis in the absence of confounding factors due to joint inflammation. Identifying downstream events that are common in the ankylosing process of *ank/ank* mice will lead to potential therapeutic targets for the human disease. These mutant mice will provide an experimental platform that enables modeling and testing of novel antiankylosis treatment strategies. Further, understanding the underlying mechanisms of the *ank/ank* phenotypes would improve our knowledge of postnatal articular cartilage homeostasis and may shed new light on pathogenic events in rheumatic diseases associated with chondrocyte hypertrophy and pathological new bone formation.

Our study has some limitations. It remains unclear whether there were any abnormal changes in the expression of Wnt proteins (such as Wnt5a)/Wnt agonists (such as R-spondins) or Wnt antagonists (such as SOST and DKK-1) in *ank/ank* mice that might contribute to activation of ß-catenin signaling. An in-depth assessment is warranted to address this issue. In addition, it is important to investigate whether increased chondrocyte hypertrophy and activation of ß-catenin signaling is a direct or indirect effect of loss of *Ank* function in the mutant mice.

We detected 2 novel *in vivo* abnormalities relating to the progressive ankylosis phenotype of *ank/ank* mice: (1) hypertrophic chondrocytes are aberrantly present in *ank/ank* articular UC; and (2) ß-catenin signaling is activated in *ank/ank* joints as evidenced by nuclear localization of ß-catenin, and higher ß-gal signals in the paw joints of *TOPGAL ank/ank* mice, likely due to fewer axin2 proteins in *ank/ank* chondrocytes. Our findings suggest that aberrant chondrocyte maturation and activation of ß-catenin signaling underlie joint ankylosis in *ank/ank* mice.

ACKNOWLEDGMENT

We are thankful for the skilled technical assistance of Gordana Kuruzar and Muntajib Alhaq, MLT, for the histological preparation, and Ruoyu Ni, BMed, MLT, for his assistance with immunohistochemistry, and Eric Gracey for photography.

REFERENCES

1. Ho AM, Johnson MD, Kingsley DM. Role of the mouse ank gene in control of tissue calcification and arthritis. Science 2000;289:265-70.
2. Goding JW, Grobben B, Slegers H. Physiological and pathophysiological functions of the ectonucleotide pyrophosphatase/phosphodiesterase family. Biochim Biophys Acta 2003;1638:1-19.
3. Terkeltaub RA. Inorganic pyrophosphate generation and disposition in pathophysiology. Am J Physiol Cell Physiol 2001;281:C1-11.
4. Hakim FT, Cranley R, Brown KS, Eanes ED, Harne L, Oppenheim JJ. Hereditary joint disorder in progressive ankylosis (ank/ank) mice. I. Association of calcium hydroxyapatite deposition with inflammatory arthropathy. Arthritis Rheum 1994;27:1411-20.
5. Gurley KA, Chen J, Guenther C, Nguyen ET, Rountree RB, Schoor M, et al. Mineral formation in joints caused by complete or joint-specific loss of ANK function. J Bone Miner Res 2006;21:1238-47.
6. Yamane S, Cheng E, You Z, Reddi AH. Gene expression profiling of mouse articular and growth plate cartilage. Tissue Eng 2007;13:2163-73.
7. Harmey D, Hessle L, Narisawa S, Johnson KA, Terkeltaub R, Millán JL. Concerted regulation of inorganic pyrophosphate and osteopontin by akp2, enpp1 and ank: An integrated model of the pathogenesis of mineralization disorders. Am J Pathol 2004;164:1199-209.
8. Wang J, Wang C, Tsui HW, Las Heras F, Cheng EY, Iscove NN, et al. Microcytosis in ank/ank mice and the role of ANKH in promoting erythroid differentiation. Exp Cell Res 2007;313:4120-9.
9. Kirsch T, Kim HJ, Winkles JA. Progressive ankylosis gene (ank) regulates osteoblast differentiation. Cells Tissues Organs 2009;189:158-62.
10. Kim HJ, Minashima T, McCarthy EF, Winkles JA, Kirsch T. Progressive ankylosis protein (ANK) in osteoblasts and osteoclasts controls bone formation and bone remodeling. J Bone Miner Res 2010;25:1771-83.
11. Zaka R, Dion A, Kusnierz A, Bohensky J, Srinivas V, Freeman T, et al. Oxygen tension regulates the expression of ANK (progressive ankylosis) in an HIF-1-dependent manner in growth plate chondrocytes. J Bone Miner Res 2009;24:1869-78.
12. Cailotto F, Bianchi A, Sebillaud S, Venkatesan N, Moulin D, Jouzeau JY, et al. Inorganic pyrophosphate generation by transforming growth factor-beta-1 is mainly dependent on ANK induction by Ras/Raf-1/extracellular signal-regulated kinase pathways in chondrocytes. Arthritis Res Ther 2007;9:R122.
13. Hens JR, Wilson KM, Dann P, Chen X, Horowitz MC, Wysolmerski JJ. TOPGAL mice show that the canonical Wnt signaling pathway is active during bone development and growth and is activated by mechanical loading in vitro. J Bone Miner Res 2005;20:1103-13.
14. Sampson HW. Spondyloarthropathy in progressive ankylosis (ank/ank) mice: morphological features. Spine 1988;13:645-9.
15. Wang G, Woods A, Sabari S, Pagnotta L, Stanton LA, Beier F. RhoA/ROCK signaling suppresses hypertrophic chondrocyte differentiation. J Biol Chem 2004;279:13205-14.
16. Wang J, Tsui HW, Beier F, Pritzker KP, Inman RD, Tsui FW. The ANKH DeltaE490 mutation in calcium pyrophosphate dihydrate crystal deposition disease (CPPDD) affects tissue non-specific alkaline phosphatase (TNAP) activities. Open Rheum J 2008; 2:25-32.
17. Church V, Nohno T, Linker C, Marcelle C, Francis-West P. Wnt regulation of chondrocyte differentiation. J Cell Sci 2002;115(Part 24):4809-18.
18. Chun JS, Oh H, Yang S, Park M. Wnt signaling in cartilage development and degeneration. BMB Rep 2008;41:485-94.

19. Zhu M, Tang D, Wu Q, Hao S, Chen M, Xie C, et al. Activation of beta-catenin signaling in articular chondrocytes leads to osteoarthritis-like phenotype in adult beta-catenin conditional activation mice. J Bone Miner Res 2009;24:12-21.
20. Kikuchi A. Roles of axin in the Wnt signaling pathway. Cell Signal 1999;11:777-88.
21. Salic A, Lee E, Mayer L, Kirschner MW. Control of beta-catenin stability: Reconstitution of the cytoplasmic steps of the wnt pathway in Xenopus egg extracts. Mol Cell 2000;5:523-32.
22. Lee E, Salic A, Kruger R, Heinrich R, Kirschner MW. The role of APC and axin derived from experimental and theoretical analysis of the Wnt pathway. PloS Biol 2003;1:E10.
23. Dao DY, Yang X, Flick LM, Chen D, Hilton MJ, O'Keefe RJ. Axin2 regulates chondrocyte maturation and axial skeletal development. J Orthop Res 2010;18:89-95.
24. Cailotto F, Sebillaud S, Netter P, Jouzeau JY, Bianchi A. The inorganic pyrophosphate transporter ANK preserves the differentiated phenotype of articular chondrocyte. J Biol Chem 2010;285:10572-82.
25. Dao DY, Yang X, Chen D, Zuscik M, O'Keefe RJ. Axin1 and Axin2 are regulated by TGF-ß and mediate cross-talk between TGF-ß and Wnt signaling pathways. Ann NY Acad Sci 2007;1116:82-99.
26. Yang X, Chen L, Xu X, Li C, Huang C, Deng CX. TGF-beta/Smad3 signals repress chondrocyte hypertrophic differentiation and are required for maintaining articular cartilage. J Cell Biol 2001;153:35-46.
27. Serra R, Johnson M, Filvaroll EH, LaBorde J, Sheehan DM, Derynck R, et al. Expression of a truncated kinase-defective TGF-ß type II receptor in mouse skeletal tissue promotes terminal chondrocyte differentiation and osteoarthritis. J Cell Biol 1997;139:541-2.
28. Corr M. Wnt-beta-catenin signaling in the pathogenesis of osteoarthritis. Nat Clin Pract Rheumatol 2008;4:550-6.
29. Johnson K, Terkeltaub R. Upregulated ank expression in osteoarthritis can promote both chondrocyte MMP-13 expression and calcification via chondrocyte extracellular PPi excess. Osteoarthritis Cartilage 2004;12:321-35.
30. Zhu M, Chen M, Zuscik M, Wu Q, Wang YJ, Rosier RN, et al. Inhibition of beta-catenin signaling in articular chondrocytes results in articular cartilage destruction. Arthritis Rheum 2008;58:2053-64.
31. Schwaninger R, Rentsch CA, Wetterwald A, van der Horst G, van Bezooijen RL, van der Pluijm G, et al. Lack of noggin expression by cancer cells is a determinant of the osteoblast response in bone metastases. Am J Pathol 2007;170:160-75.
32. Thudi NK, Martin CK, Murahari S, Shu ST, Lanigan LG, Werbeck JL, et al. Dickkopf-1 (DKK-1) stimulated prostate cancer growth and metastasis and inhibited bone formation in osteoblastic bone metastases. Prostate 2010;71:615-25.
33. Sweet HO, Green MC. Progressive ankylosis, a new skeletal mutation in the mouse. J Heredity 1981;72:87-93.
34. Tsui HW, Inman RD, Paterson AD, Reveille JD, Tsui FWL. ANKH variants associated with ankylosing spondylitis: gender differences. Arthritis Res Ther 2005;7:R513-25.
35. Furuichi T, Maeda K, Chou CT, Liu YF, Liu TC, Miyamoto Y, et al. Association of the MSX2 gene polymorphisms with ankylosing spondylitis in Japanese. J Hum Genet 2008;53:419-24.
36. Timms AE, Zhang Y, Bradbury L, Wordsworth BP, Brown MA. Investigation of the role of ANKH in ankylosing spondylitis. Arthritis Rheum 2003;48:2898-902.
37. Guo Y, Hsu DKW, Feng SY, Richards CM, Winkles JA. Polypeptide growth factors and phorbol ester induce progressive ankylosis (ank) gene expression in murine and human fibroblasts. J Cell Biochem 2001;84:27-38.
38. DePrimo SE, Diehn M, Nelson JB, Reiter RE, Matese J, Fero M, et al. Transcriptional programs activated by exposure of human prostate cancer cells to androgen. Genome Biol 2002;3:32.1-32.12.
39. Daoussis D, Liossis SC, Solomou EE, Tsanaktsi A, Bounia K, Karampetsou M, et al. Evidence that Dkk-1 is dysfunctional in ankylosing spondylitis. Arthritis Rheum 2010;62:150-8.
40. Uderhardt S, Diarra D, Katzenbeisser J, David JP, Zwerina J, Richards W, et al. Blockage of Dickkopf (DKK)-1 induces fusion of sacroiliac joints. Ann Rheum Dis 2010;69:592-7.
41. Appel H, Ruiz-Heiland G, Listing J, Zwerina J, Herrmann M, Mueller R, et al. Altered skeletal expression of sclerostin and its link to radiographic progression in ankylosing spondylitis. Arthritis Rheum 2009;60:3257-62.
42. van der Heijde D, Landewe R, Einstein S, Ory P, Vosse D, Ni L, et al. Radiographic progression of ankylosing spondylitis after up to two years of treatment with etanercept. Arthritis Rheum 2008;58:1324-31.
43. van der Heijde D, Landewe R, Baraliakos X, Houben H, van Tubergen A, Williamson P, et al. Radiographic findings following two years of infliximab therapy in patients with ankylosing spondylitis. Arthritis Rheum 2008;58:3063-70.
44. Claudepierre P, Wendling D. Are inflammation and ossification on separate tracks in ankylosing spondylitis? Joint Bone Spine 2008;75:520-2.